Resonant hydrogenic impurity states and $1s-2p_0$ transitions in coupled double quantum wells

S. T. Yen*
Department of Electronics Engineering, National Chiao Tung University, Hsinchu 30050, Taiwan, Republic of China
(Received 8 February 2003; revised manuscript received 2 June 2003; published 21 October 2003)

Calculations of the $1s$ and resonant $2p_0$ states of a shallow donor in double-quantum-well structures are performed. The variational method is used to calculate the localized part of the impurity states, taking into account the effect of intersubband mixing. The resonance coupling of the $2p_0$ state with the first subband is then dealt with using the Green function technique. The results show that for an asymmetric double-quantum-well structure the $1s$ state has a maximum binding energy as the donor is around the center of the wider well while the $2p_0$ state has in general a maximum binding energy as the donor is in the narrower well. The resonant coupling of the $2p_0$ state is stronger for the structures with a stronger intersubband mixing, where the $2p_0$ energy level is closer to the first subband bottom. The resonance-induced broadening of the $2p_0$ state can be as large as 6 meV, corresponding to a lifetime of ~ 0.1 ps. The resonance in general causes a negligibly small blueshift but can give a redshift of the order of 1 meV when the resonance is strong. A phase transition of the $2p_0$ state can occur from the resonant nature to the bound nature by modulation of the interwell coupling. The $1s-2p_0$ transition energy is also calculated. The possibility of population inversion between the $1s$ and $2p_0$ states is discussed.

DOI: 10.1103/PhysRevB.68.165331 PACS number(s): 73.20.Hb

I. INTRODUCTION

In the last two decades, there has been considerable attention given to shallow impurities confined to quasi-two-dimensional (quasi-2D) systems formed by $GaAs/Al_xGa_{1-x}As$ epitaxial layers[1–22] because of their technological importance in electronic and optoelectronic devices as well as their intrinsic physical interest. Numerous theoretical investigations have been performed with[6,16–22] or without[1–5,7–15] an external magnetic field to understand the physics of the hydrogenic impurity states in quantum wells (QW's). Due to the quite large difference in symmetry between the impurity Coulomb potential and rectangular QW potential, the problem of impurity states in QW's may not be exactly solvable and its solutions are in general obtained by variational calculations with localized trial functions. The calculations have been mostly limited to the ground states $1s$ and some low-lying excited states such as $2p_0$, $2p_{\pm 1}$, $3d_0$, $3d_{\pm 1}$, $3d_{\pm 2}$, etc., in the usual spectroscopic notation.[20] The states $1s$, $2p_{\pm 1}$, $3d_{\pm 2}$, etc., have zero nodes along the growth axis (the z axis), in similarity to the states in the lowest subband. In the absence of magnetic fields, such states always lie below the lowest subband (regardless of the QW width) and therefore have been regarded as associated with the lowest subband. Similarly, the $2p_0$ and $3d_{\pm 1}$ states are associated with the second subband because of their nodal property along the z axis, similar to the states in the second subband. With the QW thickness changing, the energy levels of the states move with the associated subband and may overlap with the lowest subband if the QW is sufficiently narrow.[3–5] In the same rule, the $3d_0$ state, associated with the third subband, may overlap in energy with the lowest two subbands. In a real case these states are unbound and are describable by the Fano formulations[23] in which the resonant interaction is treated between a discrete energy level and one or more continua of states that overlap with the energy level. The Fano resonance is not a new problem; it has been frequently studied in various fields of physics, particularly in atomic, molecular, and solid-state physics. Such a resonance can lead to an energy shift and broadening of the resonant state. The resonant impurity states in bulk semiconductors have been studied, for instance, by Bassani *et al.*[24]

The resonance of impurity states confined to QW's was first pointed out by Priester *et al.*[10] and later was investigated, both theoretically[12–14] and experimentally,[11] in several works. In the studies of Priester *et al.*[10] and Jayakumar *et al.*,[12] the calculations were limited to the on-center impurity—the impurity at the center of the QW. The localized part of each impurity state was determined by a single subband to which the impurity state is attached, with the intersubband mixing neglected.[10,12] The resonant effect was then considered using the Green function technique, equivalent to the treatment of the Fano model.[23] Because of neglecting intersubband mixing, their calculations will be valid quantitatively only for the impurity in a sufficiently narrow QW where its binding energy is much smaller than the energy separation between its corresponding subband and the nearest higher one. For the on-center impurity, the parity difference causes no resonant coupling between the $2p_0$ state and the lowest subband; consequently, the $3d_0$ state is the lowest resonant state in resonance with the lowest subband. Calculated results showed that the resonance effect causes a negligibly weak shift and broadening of the $3d_0$ state (both are of the order of 0.1 meV). The resonance of the $2p_0$ state was first theoretically investigated by Yen, with varying the impurity position in the QW and taking into acount the intersubband mixing.[14] The resulting energy broadening has been found capable of ~ 3meV (corresponding to a lifetime of ~ 0.1ps) for the impurity midway between the center and the edge of a 400-Å QW. It is expected that such a predominant resonance would allow a more resolvable experimental observation, compared to the resonance of $3d_0$ state, under the environment of various intrinsic scatterings.

There have been a number of studies of impurity states in

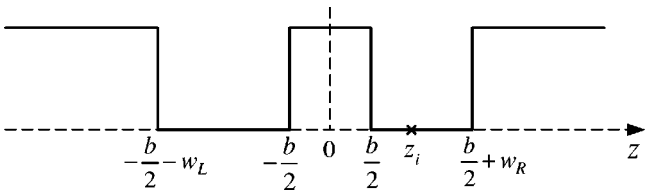

FIG. 1. Schematic illustration of the GaAs/$Al_xGa_{1-x}As$ CDQW structure consisting of a GaAs left well of thickness w_L and a GaAs right well of thickness w_R, separated and sandwiched by $Al_xGa_{1-x}As$ barriers. The interwell barrier is of thickness b. The origin is taken at the midpoint of the interwell barrier. The donor is at $z=z_i$.

coupled double quantum wells (CDQW's) consisting of two QW's separated by a thin barrier.[15–19] These investigations were totally focused on the localized states ($1s$ and $2p_{\pm 1}$) associated with the lowest subband, in no external field,[15] in a magnetic field,[16–18] or simultaneously in an electric and a magnetic fields.[19] In a CDQW structure, concurrent effects of quantum confinment and interwell tunneling on the impurity states lead to a rich variation of the binding energy, depending on the overlap between the impurity Coulomb potential and the distribution of the electron density which is a function of the impurity position, the well thickness, the barrier thickness, the ratio of the thicknesses of the two QW's, and also the external fields.

In this paper, the $2p_0$ resonant donor state in GaAs/$Al_xGa_{1-x}As$ CDQW's is investigated. We calculate, based on the theory in Ref. 14, the variations of the lifetime broadening, the energy shift (due to the resonance effect), and the binding energy of the $2p_0$ state in CDQW structures, as functions of the impurity position and well thickness, for different interwell coupling. Because of the strong resonant coupling of the $2p_0$ state with the continuum of the lowest subband, it is expected to be a potential candidate for hot electron traps in the mechanism leading to a negative differential conductance[24] and serve as the upper state for intraimpurity population inversion between the $1s$ and $2p_0$ states for terahertz-stimulated emission.[25] Therefore, we also calculate the $1s-2p_0$ transition energy for the donor in CDQW structures as a function of the impurity position and the well width. In Sec. II we present briefly the calculation techiques. Calculated results and discussion are presented in Sec. III. Finally, a summary of the results and a conclusion are drawn in Sec. IV.

II. CALCULATION METHOD

The CDQW structure considered in this study, as schematically shown in Fig. 1, consists of two GaAs wells, the left one being of thickness w_L and the right one being of thickness w_R, saparated by an $A_xGa_{1-x}As$ barrier of thickness b. The whole structure is assumed sandwiched by two semi-infinite $Al_xGa_{1-x}As$ barriers. The origin of the coordinates is taken to be at the midpoint of the interwell barrier and z_i denotes the z coordinate of the hydrogenic donor at an arbitrary position. The in-plane radial coordinate of the donor location is assumed to be $\rho=0$.

The problem of impurity states in CDQW's is dealt with mainly based on the approaches in Ref. 14 with a slight modification. According to the multisubband theory in Ref. 14, the $1s$ donor state ψ_{1s} in a 2D system is totally localized while the $2p_0$ state ψ_{2p_0} may be unbound due to the resonance interaction. Therefore, ψ_{2p_0} is expressed in a combination of a localized part $\psi_{2p_0}^{(B)}$ and an extending part $\psi_{2p_0}^{(X)}$: $\psi_{2p_0}=\psi_{2p_0}^{(B)}+\psi_{2p_0}^{(X)}$. The localized functions ψ_{1s} and $\psi_{2p_0}^{(B)}$ are obtained by the variational method. To find proper trial functions for ψ_{1s} and $\psi_{2p_0}^{(B)}$, we note first from the multisubband theory[14] that ψ_{1s} is an element of a function space $\mathcal{S}_{\geqslant 1}$ which is a Hilbert space with all subband state functions $\psi_{n\mathbf{k}}$ of the corresponding impurity-free 2D system (where n is the subband index and $\mathbf{k}$ is an in-plane wave vector) as the basis vectors. Also, $\psi_{2p_0}^{(B)}$ is an element of $\mathcal{S}_{\geqslant 2}$ and $\psi_{2p_0}^{(X)}$ is an element of $\mathcal{S}_1$, where $\mathcal{S}_{\geqslant \nu}$ represents the function space with the subband state functions $\psi_{n\mathbf{k}}$ ($n\geqslant\nu$) above the $(\nu-1)$th subband as the basis vectors and $\mathcal{S}_\nu$ represents the function space with the functions $\psi_{\nu\mathbf{k}}$ in the νth subband as the basis vectors. Therefore, $\mathcal{S}_{\geqslant 1}=\mathcal{S}_{\geqslant 2}+\mathcal{S}_1$. As a matter of fact, ψ_{1s} must be the extremal giving the global minimum of the functional $E[\psi]$ of the expectation value of the energy $E[\psi]=\langle\psi|H|\psi\rangle/\langle\psi|\psi\rangle$ for $\psi\in\mathcal{S}_{\geqslant 1}$, since ψ_{1s} is the ground state of the 2D system with the impurity, which is described by the Hamiltonian H where

$$H=H_0+V_c(\mathbf{r}), \tag{1a}$$

$$V_c(\mathbf{r})=-\frac{2}{\epsilon\sqrt{\rho^2+(z-z_i)^2}}. \tag{1b}$$

Here H_0 is the impurity-free Hamiltonian of the CDQW, V_c is the Coulomb potential energy due to the positive charge of the donor, and ϵ is the static dielectric constant of the material. We neglect the difference in dielectric constant between the well and barrier layers. The electron is at the position $\mathbf{r}=(\boldsymbol{\rho},z)$ where ρ is the in-plane radial vector and z is the z-component coordinate of the electron. The effective atomic units have been adopted in Eq. (1). The energy and length are in units of the effective Rydberg and effective Bohr radius, respectively, of the material (GaAs) making up the well.[14] Similarly, the localized function $\psi_{2p_0}^{(B)}$ is the extremal giving the minimum of the expectation value of the energy in the space $\mathcal{S}_{\geqslant 2}$: $E[\psi]=\langle\psi|H|\psi\rangle/\langle\psi.\,|\psi\rangle$ for $\psi\in\mathcal{S}_{\geqslant 2}$. For admissible functions restricted within $\mathcal{S}_{\geqslant 2}$, $\psi_{2p_0}^{(B)}$ can therefore be regarded as the ground state of the Hamiltonian.[14] On the contrary, for functions in the total space $\mathcal{S}_{\geqslant 1}$, $\psi_{2p_0}^{(B)}$ is no longer stationary and must be corrected with the part $\psi_{2p_0}^{(X)}$.

Based on the argument above, we calculate variationally ψ_{1s} and $\psi_{2p_0}^{(B)}$ using the trial functions which are elements of $\mathcal{S}_{\geqslant 1}$ and $\mathcal{S}_{\geqslant 2}$, respectively. We take the trial functions in the form[14]

$$\psi_\nu=\sum_{n\geqslant\nu}\sum_l C_{nl}e^{-\alpha_l\rho^2}f_n(z), \tag{2}$$

where $\nu=1$ for ψ_{1s} and $\nu=2$ for $\psi^{(B)}_{2p_0}$. Here $f_n(z)$ is the z-dependent part of the subband function $\psi_{n\mathbf{k}}=e^{i\mathbf{k}\cdot\rho}f_n(z)/\sqrt{A}$ (A being the area of the CDQW) which satisfies the impurity-free Schrödinger equation $H_0\psi_{n\mathbf{k}}=E_{n\mathbf{k}}\psi_{n\mathbf{k}}$, $E_{n\mathbf{k}}$ being the corresponding eigenvalue. Obviously, $\psi_1\in\mathcal{S}_{\geqslant 1}$ and $\psi_2\in\mathcal{S}_{\geqslant 2}$. It should be pointed out that the trial functions ψ_1 and ψ_2 in the form (2) are not necessarily orthogonal since ψ_2 is the trial function for $\psi^{(B)}_{2p_0}$ which is only the localized part of the $2p_0$ state ψ_{2p_0}. A more detailed discussion about the orthogonality between the $1s$ and $2p_0$ states can be found in Ref. 14. For a given set of α_l, minimizing $E[\psi_\nu]$ by varying C_{nl} gives a set of eigenvalue equations $\partial E/\partial C_{nl}=0$ $(n=\nu,\nu+1,\ldots;\ l=1,2,\ldots)$, which determines the minimal expectation values and simultaneously the corresponding coefficients C_{nl}. By further varying the nonlinear parameters α_l, we have more degrees of freedom to obtain a lower minimal E which corresponds to a more accurate solution. The set of α_l leading to the minimum energies, E_{1s} or $E^{(B)}_{2p_0}=\min_{\psi_\nu}E[\psi_\nu]$, gives the best solutions for ψ_{1s} and $\psi^{(B)}_{2p_0}$ in the framework of the trial function (2). The binding energies of the $1s$ and $2p_0$ states are then determined by the energy differences $E_{B,1s}=E_{1,\mathbf{k}=0}-E_{1s}$ and $E_{B,2p_0}=E_{2,\mathbf{k}=0}-E^{(B)}_{2p_0}$, respectively.

It is worth giving a discussion about the applicability restrictions of the trial function (2). The localized functions ψ_{1s} and $\psi^{(B)}_{2p_0}$ can be described by the trail function (2) with an accuracy depending on the numbers of Gaussian orbitals $e^{-\alpha_l\rho^2}$ and subband functions $f_n(z)$ that are included in the trial function (2). For an impurity in a very wide (>400 Å) or very narrow (<30 Å) well such that a lot of subbands are close in energy to the impurity state of interest, one must include many subband functions $f_n(z)$ in the trial function (2) to obtain an accurate result. Fortunately, increasing the number of subband functions means an increase in the number of linear variational parameters C_{nl}. In this case, one has simply to diagonize larger-rank matrices.

Once the localized part $\psi^{(B)}_{2p_0}$ is obtained, the resonance coupling between $\psi^{(B)}_{2p_0}$ and the continuum of the lowest subband states $\psi_{1,\mathbf{k}}$ is treated with the Green function technique. The resulting partial density of states (DOS) of the $2p_0$ resonant state ψ_{2p_0} can be written in the form of[14]

$$n_{2p_0}(E)=-\frac{1}{\pi}\mathrm{Im}\frac{1}{F(E)+i\Gamma(E)}, \tag{3a}$$

$$F(E)=E-E^{(B)}_{2p_0}-\frac{1}{\pi}P\int_{E_{1,\mathbf{k}=0}}^{\infty}\frac{\Gamma(E')}{E-E'}dE', \tag{3b}$$

$$\Gamma(E)=\pi\sum_{\mathbf{k}}\ |\langle\psi^{(B)}_{2p_0}|V_c|\psi_{1,\mathbf{k}}\rangle|^2\delta(E-E_{1,\mathbf{k}})$$

$$=\begin{cases}\dfrac{A}{4}|\langle\psi^{(B)}_{2p_0}|V_c|\psi_{1,k=\sqrt{E-E_{1,\mathbf{k}=0}}}\rangle|^2 & \text{for}\quad E\geqslant E_{1,\mathbf{k}=0}\\ 0 \quad \text{for}\quad E<E_{1,\mathbf{k}=0}.\end{cases} \tag{3c}$$

Here Px^{-1} means to take the Cauchy principal value of x^{-1}. The resonance energy E_{2p_0} of the $2p_0$ state is obtained by finding the peak position of the partial DOS spectrum $n_{2p_0}(E)$. The broadening width of the $2p_0$ state is here defined as the full width of half maximum (FWHM) of the partial DOS spectrum, different from that in Ref. 14. The DOS spectrum is of a Lorenzian shape if its width is much smaller than the energy difference $E_{2p_0}-E_{1,\mathbf{k}=0}$; in this case the FWHM can be well approximated by $2\Gamma(E_{2p_0})$. It reflects the capture time of an electron from the lowest subband states $\psi_{1,\mathbf{k}}$ into the $2p_0$ localized state $\psi^{(B)}_{2p_0}$ and also the escape time of an electron from the localized to the subband states. The resonance lifetime is estimated using the relation $\tau=\hbar/\mathrm{FWHM}$. The resonant coupling also causes an energy shift of $\Delta E=E_{2p_0}-E^{(B)}_{2p_0}$.

III. RESULTS AND DISCUSSION

In this section we present the calculated results for the donor states in GaAs/Al_xGa_{1-x}As CDQW structures with an interwell barrier of thickness $b=2$ nm. In the calculations, the effective mass of $Al_xGa_{1-x}As$ is assumed to be $0.0665(1+1.25x)m_e$ where m_e is the free electron mass. The barrier height at the GaAs/Al_xGa_{1-x}As interfaces is determined from the relation $\Delta E_g=1.36x+0.22x^2$ eV with 60% conduction-band offset. The static dielectric constant ϵ is taken as 12.5. These parameters are intentionally taken the same as those in Ref. 19 to compare some of our results with those in Ref. 19.

In the variational calculation, we use nine subbands $f_n(z)$ ($n=1$–9 for ψ_{1s} and $n=2$–10 for $\psi^{(B)}_{2p_0}$) and five Gaussian orbitals $e^{-\alpha_l\rho^2}$ ($l=1$–5) for the trial functions expressed in Eq. (2). The nine subbands are all discrete even if some of them are above the barrier in energy since we use the CDQW structures bounded by two infinitely high potential walls (60 nm apart) to simulate the real structures.[14] It has been previously checked that the infinitely high potential walls are far apart from each other such that the impurity states of interest will not be affected by the artificial enclosure. The five parameters α_l are taken in the form of $\alpha_l=\alpha+0.25(l-1)^3$ where α is determined variationally.[14] This set of α_l is found capable of giving accurate binding energy by comparing the binding energies obtained using a variety of sets of α_l in the variational calculation.

Figure 2 shows the binding energies of the $1s$ state ($E_{B,1s}$) and $2p_0$ state ($E_{B,2p_0}$) as functions of the impurity position z_i in various CDQW structures. In Fig. 2(a), the curves are for the structures consisting of a GaAs left well of thickness $w_L=10$ nm and a GaAs right well of thickness varying from 3 to 10 nm ($w_R=3$, 5, 7, 9, 10 nm), separated by a 2-nm $Al_{0.2}Ga_{0.8}As$ interwell barrier, and then sandwiched by $Al_{0.2}Ga_{0.8}As$ barriers. (See Fig. 1.) For Fig. 2(b), the structures are similar to those for Fig. 2(a) except that $Al_{0.3}Ga_{0.7}As$ is used for the barriers. Also, we replace the curves for $(w_L,w_R)=(10,7)$ nm with those for (5,2.5) nm to make a comparison of the $1s$ binding energy of the (5,2.5)-nm CDQW with that in Fig. 4(a) of Cen *et al.*[19] The

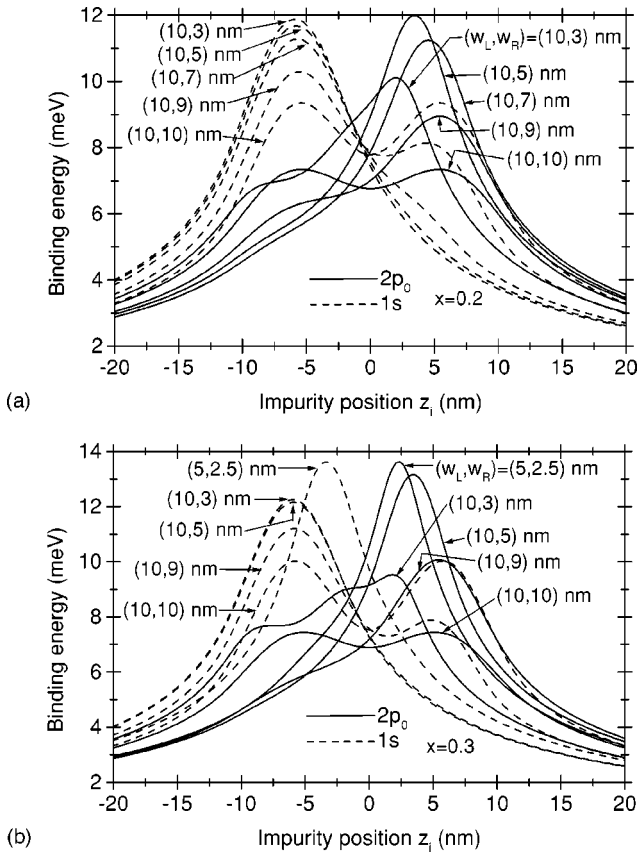

FIG. 2. The binding energies of the $1s$ state (dashed curves) and the $2p_0$ state (solid curves) vs the impurity position z_i for CDQW structures with (a) $Al_{0.2}Ga_{0.8}As$ barriers and (b) $Al_{0.3}Ga_{0.7}As$ barriers. The structures considered in (a) have a left well of thickness $w_L=10$ nm and a narrower right well of thickness varying from 3 to 10 nm ($w_R=3$, 5, 7, 9, 10 nm). The structures in (b) are similar to those in (a), except that the structure of $(w_L,w_R)=(10,7)$ nm is replaced by that of (5,2.5) nm. All the structures have an interwell barrier of thickness $b=2$ nm.

results are in excellent agreement. It is found that the $1s$ state has a maximum binding energy as the impurity is around the center of the left wider well for asymmetric CDQW structures. This is because there is a larger likelihood of finding the electron of the lowest subband states in the wider well. Since the $1s$ state is mostly composed of the lowest subband states $\psi_{1,\mathbf{k}}$ ($\propto f_1$), the impurity in the wider well enhances the Coulomb potential compared to the impurity in the narrower well. A larger overlap between the electron distribution and the Coulomb potential leads to a larger binding energy. This can also explain that the peak binding energy of the $1s$ state increases as the right well thickness decreases. With the right narrower well thickness decreasing, the probability of finding the electron in the right well reduces and part of it transfers to the left well through interwell tunneling; this enhances the $1s$ binding energy as the impurity stays in the left wider well. (The change in the distribution of the electron probability density can also be understood from the viewpoint of intersubband mixing between the first and second subbands.) For the symmetric structure $[(w_L,w_R)=(10,10)\text{nm}]$, the electron density has a symmetric distribution, resulting in two lowest peaks of the binding energy. Similarly, the $2p_0$ state has a maximum binding energy as the impurity is around the center of the right narrower well, except for the structures (10,3) nm, since the $2p_0$ state is mostly composed of the second subband states $\psi_{2,\mathbf{k}}$ ($\propto f_2$) in which the electron is more likely to stay in the narrower well. For the symmetric structure, there is equal likelihood of finding the electron of the second subband states in the two wells. Thus we have a symmetric variation of the $2p_0$ binding energy with the impurity position. With the right narrower well thickness decreasing, the electron density $|f_2(z)|^2$ initially has a tendency to being localized in the right well because of the reduction of the intersubband mixing and, consequently, the $2p_0$ peak binding energy increases. Further decreasing the right well thickness then causes the electron density to spread out of the right well into the barriers and the left wider well since the second quantized level is pushed up close to the third and other higher subbands (a peculiarity in CDQW), increasing the mixing of the second subband with the higher subbands. This explains the reduction of the $2p_0$ binding energy as the right well thickness decreases from $(w_L,w_R)=(10,5)$ to (10,3)nm. Furthermore, the $2p_0$ peak binding energy for the (10,3)-nm structures occurs at a position deviating significantly from the center of the right narrower well. The results indicate that the effect of intersubband mixing is important in accurate calculations of the $2p_0$ state in a CDQW structure. We also find from Fig. 2(b) that the effect of intersubband mixing is smaller on the $2p_0$ state in the (5,2.5)-nm structure than in the (10,3)-nm structure because of the difference in the left wider well thickness.

Figure 3 shows the FWHM of the patial DOS spectrum of the $2p_0$ state induced by the resonance coupling as a function of the impurity position z_i for the CDQW structures consisting of a 10-nm left well and a right narrower well of various thicknesses ($w_R=3,5,7,9,10$ nm), separated and sandwiched by (a) $Al_{0.2}Ga_{0.8}As$ barriers and (b) $Al_{0.3}Ga_{0.7}As$ barriers. The interwell barrier layers are still of thickness $b=2$ nm. It is found from Fig. 3(a) that for the structures with $Al_{0.2}Ga_{0.8}As$ barriers each curve exhibits two peaks as the impurity is around the centers of both the left and the right wells, except for the (10,3)-nm structure. The variation of the $2p_0$ spectrum width can be well explained by means of the matrix elements in Eq. (3c). Since the matrix element is of the Coulomb potential between $\psi_{1,\mathbf{k}}$ and $\psi^{(B)}_{2p_0}$, according to their nodal properties along the z axis, we expect that a local minimum of the spectrum width occurs as the impurity is around the midpoint of the whole structure, in agreement with the result in Fig. 3(a). This also explains the two peaks of each curve. It is found that the stronger resonance occurs in the (10,9)-nm and (10,10)-nm CDQW structures (where the intersubband mixing is stronger) and the resonance becomes weak as the right well thickness decreases. The coupling strength $\Gamma(E_{2p_0})$ also sensitively depends on the magnitude of the wave vector, $k=\sqrt{E_{2p_0}-E_{1,\mathbf{k}=0}}$, and thus on the energy difference $E_{2p_0}-E_{1,\mathbf{k}=0}$. For a large value of k, $\psi_{1,\mathbf{k}}$ exhibits a rapid oscillation along ρ, leading to a small overlap integral of $|\langle\psi^{(B)}_{2p_0}|V_c|\psi_{1,\mathbf{k}}\rangle|$, as has also been dem-

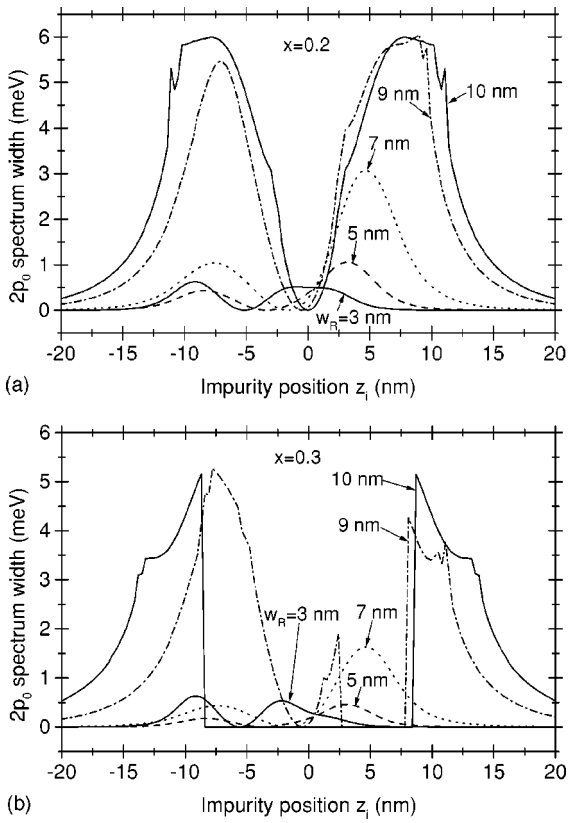

FIG. 3. The FWHM of the partial DOS spectrum of the $2p_0$ state vs the impurity position z_i for CDQW structures with a left well of thickness $w_L=10$ nm and a narrower right well of thickness varying from 3 to 10 nm ($w_R=3,5,7,9,10$ nm). The structures considered in (a) and (b) have barriers made of $Al_{0.2}Ga_{0.8}As$ and $Al_{0.3}Ga_{0.7}As$, respectively. The interwell thickness of the structures is $b=2$ nm.

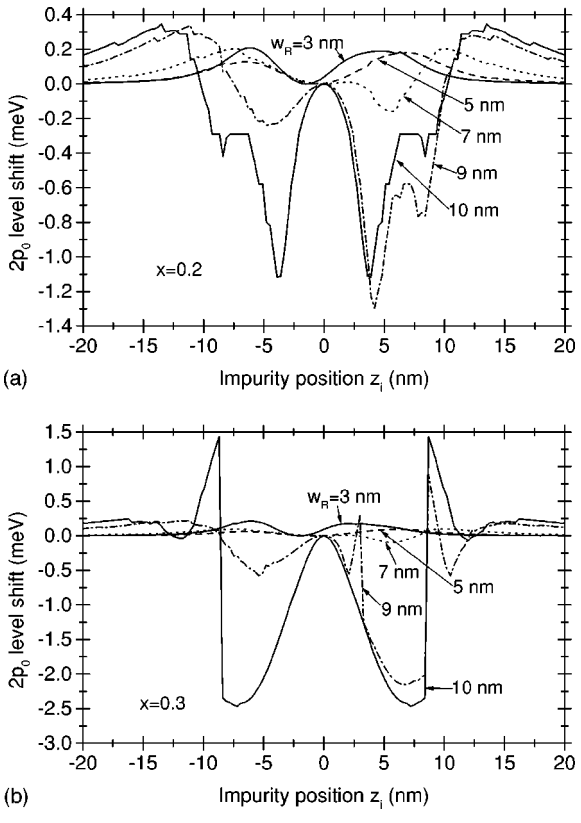

FIG. 4. The resonance-induced energy shift of the $2p_0$ state vs the impurity position z_i for CDQW structures with a left well of thickness $w_L=10$ nm and a narrower right well of thickness varying from 3 to 10 nm ($w_R=3,5,7,9,10$ nm). The structures considered in (a) and (b) have barriers made of $Al_{0.2}Ga_{0.8}As$ and $Al_{0.3}Ga_{0.7}As$, respectively. The interwell thickness of the structures is $b=2$ nm.

onstrated in Fig. 3 of Ref. 10. With the right well thickness decreasing, E_{2p_0} moves upwards with the second subband while the first subband has merely a slight change. As a result, the energy difference $E_{2p_0}-E_{1,\mathbf{k}=0}$ increases and the resonance coupling decreases with the right well thickness decreasing. It is noticed that further decreasing the right well thickness causes strong subband mixing between the second and higher subbands, as has been described above (and therefore gives a significant probability density of the second subband states in the left well), enhancing the resonance coupling as the impurity is in the left well. This explains that the left peak for the (10,3)-nm structure is higher than the (10,5)-nm structure and the right peak for the (10,3)-nm structure occurs as the impurity is at a position deviating significantly from the center of the right well.

For the CDQW structures with Al0.3$Ga_{0.7}As$ barriers, the variations of the $2p_0$ spectrum width for $w_R \leqslant 7$ nm are essentially similar to those for the structures with Al0.2$Ga_{0.8}As$ barriers, but for $w_R \geqslant 9$ nm, the behavior is quite different, as can be seen in Fig. 3(b). As the impurity position z_i is in the range from -8 to 8 nm, the $2p_0$ level for $w_R=10$ nm lies below the first subband because the weak interwell coupling results in a small separation of the lowest two subbands. The $2p_0$ state in this case becomes purely localized and the corresponding spectrum width becomes zero. Similarly, as the impurity lies at $z_i=2.5-7.5$ nm, the $2p_0$ state for $w_R=9$ nm is bound but becomes resonant as the impurity moves out of the range. Accordingly, we expect a transition from the resonant phase to the bound phase of the $2p_0$ state in a CDQW structure by modulation of the interwell coupling, which can be easily achieved by an external electric field normal to the interfaces.

Because the resonance coupling depends on the energy separation between the impurity level and the edge of the in-resonance subband, the $2p_0$ state can have a much stronger resonance strength than the $3d_0$ state. The result in Fig. 3 shows that the broadening of the $2p_0$ state can be as large as 6 meV (corresponding to a lifetime of ~ 0.1 ps), an order of magnitude larger than the $3d_0$ state.[10,12] Since such a short resonance lifetime is in general less than the lifetime due to other intrinsic scatterings, we expect that the resonance can play a predominant role in a certain of physical processes.

The energy shift of the $2p_0$ state arising from the resonance coupling is shown in Figs. 4(a) and 4(b) as a function of the impurity position z_i for the CDQW structures that are the same as in Figs. 3(a) and 3(b), respectively. The energy shift exhibits a more complicated variation with z_i, compared to the binding energy and the spectrum width. We

know from Eq. (3) that it depends on the $2p_0$ energy level E_{2p_0} and the coupling strength $\Gamma(E)$ over a range of energy. For weak coupling strength $\Gamma(E)\approx 0$, the peak of the partial DOS spectum is at $E_{2p_0}\approx E_{2p_0}^{(B)}$ and the energy shift $\Delta E = E_{2p_0} - E_{2p_0}^{(B)}$ is small. This explains the more considerable shift for a wider right well (with a stronger intersubband mixing). Since the function $\Gamma(E)$ in general monotonically decreases with E, the integral in Eq. (3b) is positive (i.e., the third term on the right gives a negative contribution) if E is not too close to the lower limit $E_{1,\mathbf{k}=0}$ of the integral; as a result, we have a blueshift for the CDQW structures with a narrow right well ($w_R = 3$–5 nm). On the other hand, for the structures with a wide right well, the energy difference $E_{2p_0} - E_{1,\mathbf{k}=0}$ is small and the energy E we are interested in is close to the lower limit $E_{1,\mathbf{k}=0}$. This causes the integral in Eq. (3b) to be negative, leading to a redshift of the resonance energy. Since the coupling for a wider right well is stronger, the energy shift in such a case is more pronounced. In the case where the $2p_0$ state is a bound state, the coupling with the first subband merely gives a correction in the binding energy, corresponding to a redshift of the $2p_0$ level. It is found that the energy shift is generally of the order 0.1 meV of magnitude for $w_R \leqslant 7$ nm, but for the case of strong coupling ($w_R \geqslant 9$ nm), the shift can be as large as being of the order 1 meV. Compared with the binding energy in Fig. 2, the energy shift is in general much smaller and can be neglected.

The electric dipole transition between the $1s$ and $2p_0$ states is allowed for electromagnetic fields polarized in the growth direction. Figure 5 shows the $2p_0$-$1s$ transition energy and $2p_0$-$E_{1,\mathbf{k}=0}$ energy difference for the impurity located at the centers of the wells as a function of the narrower right well thickness w_R, with the left wider well thickness fixed to be $w_L = 10$ nm. The curves in Figs. 5(a) and 5(b) are for the structures with barriers layers made up of $Al_{0.2}Ga_{0.8}As$ and $Al_{0.3}Ga_{0.7}As$, repectively. It is evident that the structure with a narrower right well has a larger transition energy and also a larger $E_{2p_0} - E_{1,\mathbf{k}=0}$ due to the large separation of the two lowest subbands. The $2p_0$-$1s$ transition energy lies in the far-infrared or terahertz range. Recently, a mechanism for population inversion between a resonant excited state and the ground state has been proposed for acceptors in strained bulk semiconductors.[25] In an external electric field parallel to the interfaces, electrons can be accelerated from the band edge upwards to the vicinity of the resonance enegy level. If the resonant coupling is strong, the electrons will likely be captured in the localized part of the resonant state from the band continuum. The excited resonant state is thus occupied and population inversion is achieved if the ground state is emptied due to impact ionization by the electric field. Based on a similar mechanism, we expect the possibility of population inversion between the $1s$ and $2p_0$ states in our CDQW structures by applying an electric field parallel to the interfaces. At sufficiently low temperature such that LO phonon absorption is negligibly weak, electrons can easily reach the $2p_0$ energy level through the lowest subband if the energy difference $E_{2p_0} - E_{1,\mathbf{k}=0}$ is less than the LO phonon energy ($\hbar\omega_{LO} \sim 36$ meV in GaAs). On the other hand, if $E_{2p_0} - E_{1,\mathbf{k}=0} \gg \hbar\omega_{LO}$, population inversion is difficult to achieve since LO phonon emission occurs before electrons reach the $2p_0$ energy level. It is found from the figures that the CDQW structures with a narrow right well ($w_R \leqslant 4$ nm) are not suitable for observation of the resonant scattering in transport processes.

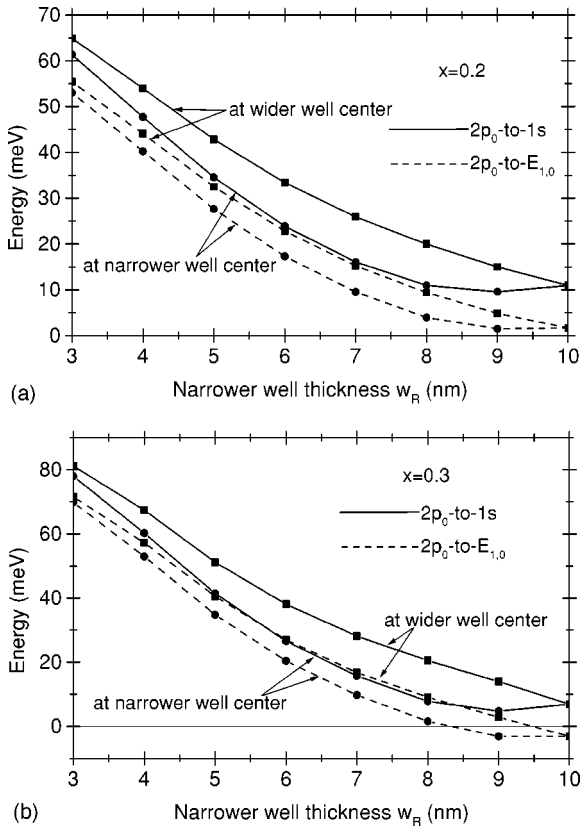

FIG. 5. The $2p_0$-$1s$ transition energy and the $2p_0 - E_{1,\mathbf{k}=0}$ energy difference vs the right well thickness w_R for the impurity locating at the centers of wells. The CDQW structures have a left well of thickness $w_L = 10$ nm and barriers made of $Al0.2Ga_{0.8}As$ in (a) and $Al_{0.3}Ga_{0.7}As$ in (b). The interwell thickness of the structures is $b = 2$ nm.

IV. CONCLUSIONS

We have presented a calculation of the $1s$ and $2p_0$ states of a shallow donor in a coupled double-quantum-well structure. The variational approach with intersubband mixing is used to calculate the $1s$ state and localized part of the $2p_0$ state. The resonance of the $2p_0$ state is considered using the Green function technique. The results show that the $1s$ state has a maximum binding energy as the donor is around the center of the wider well of the CDQW structure, while the $2p_0$ state generally has a maximum binding energy as the donor is around the center of the narrower well. The resonant coupling of the $2p_0$ state with the lowest subband is strong when the $2p_0$ energy level is close to the lowest subband bottom. The resonance can give a lifetime of ~ 0.1 ps. By modulation of the interwell coupling, the resonant nature of

the $2p_0$ state can change to the bound nature. The resonance in general causes a negligibly small blueshift of the $2p_0$ energy. However, when the $2p_0$ energy level is close to the lowest subband bottom, it may causes a redshift of the order of 1 meV. The $2p_0$-1s transition energy is also presented as a function of the narrower well thickness. The results are useful in designing a CDQW structure for experimentally observing the resonance effects of the $2p_0$ state.

ACKNOWLEDGMENT

This work was supported by the National Science Council of the Republic of China under Contract No. NSC 90-2112-M-009-054.

*Electronic address: styen@faculty.nctu.edu.tw

[1] G. Bastard, Phys. Rev. B **24**, 4714 (1981).
[2] C. Mailhiot, Y.-C. Chang, and T. C. McGill, Phys. Rev. B **26**, 4449 (1982).
[3] R. L. Greene and K. K. Bajaj, Solid State Commun. **45**, 825 (1983).
[4] S. Chaudhuri and K. K. Bajaj, Phys. Rev. B **29**, 1803 (1984).
[5] R. L. Greene and K. K. Bajaj, Phys. Rev. B **31**, 4006 (1985).
[6] R. L. Greene and K. K. Bajaj, Phys. Rev. B **31**, 913 (1985).
[7] S. Chaudhuri, Phys. Rev. B **28**, 4480 (1983).
[8] J.-B. Xia, Phys. Rev. B **39**, 5386 (1989).
[9] S. Fraizzoli, F. Bassani, and R. Buczko, Phys. Rev. B **41**, 5096 (1990).
[10] C. Priester, G. Allan, and M. Lannoo, Phys. Rev. B **29**, 3408 (1984).
[11] T. A. Perry, R. Merlin, B. V. Shanabrook, and J. Comas, Phys. Rev. Lett. **54**, 2623 (1985).
[12] K. Jayakumar, S. Balasubramanian, and M. Tomak, Phys. Rev. B **34**, 8794 (1986).
[13] A. Blom, M. A. Odnoblyudov, I. N. Yassievich, and K. A. Chao, Phys. Rev. B **65**, 155302 (2002).
[14] S. T. Yen, Phys. Rev. B **66**, 075340 (2002).
[15] H. Chen and S. Zhou, Phys. Rev. B **36**, 9581 (1987).
[16] R. Ranganathan, B. D. McCombe, N. Nguyen, Y. Zhang, M. L. Rustgi, and W. J. Schaff, Phys. Rev. B **44**, 1423 (1991).
[17] N. Nguyen, R. Ranganathan, B. D. McCombe, and M. L. Rustgi, Phys. Rev. B **44**, 3344 (1991).
[18] J. Cen and K. K. Bajaj, Phys. Rev. B **46**, 15280 (1992).
[19] J. Cen, S. M. Lee, and K. K. Bajaj, J. Appl. Phys. **73**, 2848 (1993).
[20] J.-P. Cheng and B. D. McCombe, Phys. Rev. B **42**, 7626 (1990).
[21] R. Chen, J.-P. Cheng, D. L. Lin, B. D. McCombe, and T. F. George, Phys. Rev. B **44**, 8315 (1991).
[22] J. X. Zang and M. L. Rustgi, Phys. Rev. B **48**, 2465 (1993).
[23] U. Fano, Nuovo Cimento **12**, 154 (1935); Phys. Rev. **124**, 1866 (1961).
[24] F. Bassani, G. Ladonisi, and B. Preziosi, Rep. Prog. Phys. **37**, 1099 (1974).
[25] M. A. Odnoblyudov, I. N. Yassievich, M. S. Kagan, Yu. M. Galperin, and K. A. Chao, Phys. Rev. Lett. **83**, 644 (1999).